

Accepted Manuscript

Title: Particle engineering of materials for oral inhalation by dry powder inhalers. I - Particles of sugar excipients (trehalose and raffinose) for protein delivery.

Authors: Orla Ní Ógáin, Jianhe Li, Lidia Tajber, Owen I. Corrigan, Anne Marie Healy



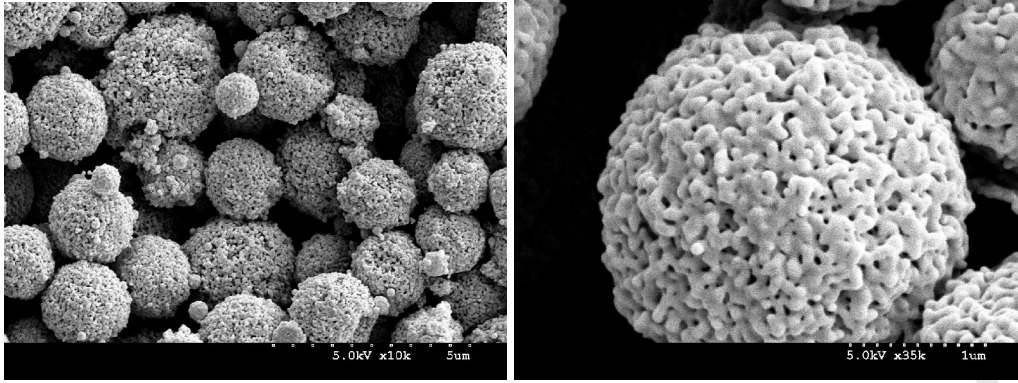
PII: S0378-5173(10)00888-4
DOI: doi:10.1016/j.ijpharm.2010.11.039
Reference: IJP 11559

To appear in: *International Journal of Pharmaceutics*

Received date: 19-8-2010
Revised date: 11-11-2010
Accepted date: 24-11-2010

Please cite this article as: Ógáin, O.N., Li, J., Tajber, L., Corrigan, O.I., Healy, A.M., Particle engineering of materials for oral inhalation by dry powder inhalers. I - Particles of sugar excipients (trehalose and raffinose) for protein delivery., *International Journal of Pharmaceutics* (2010), doi:10.1016/j.ijpharm.2010.11.039

This is a PDF file of an unedited manuscript that has been accepted for publication. As a service to our customers we are providing this early version of the manuscript. The manuscript will undergo copyediting, typesetting, and review of the resulting proof before it is published in its final form. Please note that during the production process errors may be discovered which could affect the content, and all legal disclaimers that apply to the journal pertain.



Particle engineering of materials for oral inhalation by dry powder inhalers. I - Particles of sugar excipients (trehalose and raffinose) for protein delivery.

Orla Ní Ógáin, Jianhe Li, Lidia Tajber, Owen I. Corrigan and Anne Marie Healy,
School of Pharmacy and Pharmaceutical Sciences, Trinity College Dublin, Dublin 2, Ireland.

Suggested running head: Nanoporous microparticles of sugars

Corresponding author:

Anne Marie Healy

School of Pharmacy and Pharmaceutical Sciences,

Trinity College, University of Dublin, Dublin 2, Ireland.

Phone: 00353-1-8961444

Fax: 00353-1-8962783

e-mail: healyam@tcd.ie

Accepted Manuscript

ABSTRACT

The pulmonary route of delivery offers a potential alternative to parenteral administration of peptides and proteins. Protection of protein structure is essential in both processing and storage of the final formulation. Sugars, such as trehalose and raffinose, have been employed to act as protein stabilisers. Optimisation of the aerodynamic characteristics of microparticles in dry powder inhaler formulations is critical to ensure optimum deposition of the formulation into the respiratory tract.

In the present study we examine the adaptation to hydrophilic materials, specifically the disaccharide, trehalose and the trisaccharide, raffinose, of a previously reported spray drying process for producing nanoporous microparticles (NPMPs). We also investigate the feasibility of incorporating a model protein, lysozyme, into these sugar-based NPMPs.

While spray drying raffinose or trehalose from aqueous solution or ethanol:water solutions resulted in non-porous microspheres, spray drying from a methanol:n-butyl acetate mixed solvent system resulted in microparticles which appeared to consist of an agglomeration of individual nanoparticles, i.e. nanoporous/nanoparticulate microparticles.

NPMPs of trehalose and raffinose were amorphous, with glass transition temperatures (T_gs) that were sufficiently high (124 °C and ~120 °C for trehalose and raffinose, respectively) to suggest good physical stability at room temperature and good potential to act as protein carriers and/or stabilisers.

NPMPs demonstrated improved aerosolisation properties compared to spray dried non-porous particles. The successful incorporation of lysozyme into these NPMPs at a sugar to protein weight ratio of 1:4 demonstrated the potential of these systems to act as carriers for peptide or protein drugs which could be delivered via the pulmonary route.

1. INTRODUCTION

Protein and peptide drugs are generally poorly absorbed across biological membranes. The majority of proteins and peptides are thus formulated as parenterals. The parenteral route has several disadvantages however, including patient discomfort, potential high cost and the risk of needle-stick injuries (Patton, 1997; Shoyele and Cawthorne, 2006). Less invasive and more patient-acceptable routes have been sought, and the pulmonary route has emerged as a particularly interesting and viable alternative. Advantages of the pulmonary route include a very large absorptive surface area (~80-140 m²), decreased metabolism and efflux transporter activity compared to the oral route, avoidance of first pass effect and potential for rapid onset of action (Adjei and Gupta, 1997; Patton et al., 2004; Scheuch et al., 2006).

Numerous studies have shown the feasibility of the pulmonary route for the systemic delivery of proteins and peptides. The first protein for systemic delivery via inhalation to be marketed was insulin (Exubera[®]), for the treatment of type 1 and type 2 diabetics. The formulation was a dry powder of recombinant human insulin (60%) spray-dried with excipients (mannitol, glycine, sodium citrate, sodium hydroxide) to produce a glassy amorphous material (White et al., 2005). Other proteins/peptides currently in development for pulmonary delivery include interleukin-1 for asthma, interferons for multiple sclerosis or hepatitis and calcitonin for osteoporosis (Mansell, 2007).

Where the protein/peptide to be used for pulmonary delivery is a low dose, high potency material, it may be desirable, for dry powder inhalation, to formulate with a carrier material (inert excipient) to increase the volume of powder loaded and delivered from the dry powder inhaler (DPI) device.

Protection of protein structure is critical in both processing and storage of the final formulation. The use of excipients to stabilise proteins during drying was initially adopted from freeze-drying data, and has shown considerable success also in spray-drying experiments (Lee, 2002). Sugars (particularly disaccharides), polyols, amino acids or organic salts have been used to protect native

protein structure during drying processes, including spray-drying, and also on storage. Two hypotheses are described for the mechanism of stabilisation – the glassy immobilisation hypothesis (Franks et al., 1991) and the water replacement hypothesis (Carpenter and Crowe, 1988; 1989). The glassy stabilisation hypothesis states that stabilisation is achieved by formation of an amorphous glass during drying. In the glassy state, structural changes are significantly delayed and only minor molecular motions for example rotational motions of side chains and vibrations occur (Lee, 2002). Nektar Therapeutics Pulmosol[®] technology makes use of glass stabilisation of spray-dried microparticles and forms the basis of the Exubera[®] insulin spray-dried product. In the water replacement hypothesis, stabilisation is attributed to the formation of H-bonding between the sensitive component and the excipient, when water is removed, thus maintaining the structural integrity of proteins, and membranes. An amorphous state may be important to allow maximal H-bonding between the excipient and protein (Arakawa et al, 2001).

Lactose, sucrose, trehalose and raffinose have been investigated as examples of stabilising sugars in spray-drying and other process drying experiments and against specific experimentally-induced stresses (for example liquid-solid interfacial stress) (Lee, 2002; Liao et al., 2002; Wendorf et al., 2004). Sucrose, trehalose and raffinose are non-reducing sugars and as such have the advantage that they will not undergo the Maillard browning reaction with proteins. These sugars, which tend to form amorphous glasses on spray-drying, have been shown to stabilise proteins both during processing and also on storage below the glass transition temperature (T_g) of the formulation (Lee, 2002).

We have previously reported on the use of a spray drying method to produce nanoporous microparticles (NPMPs) of two hydrophobic materials with low aqueous solubility, bendroflumethiazide (Healy et al, 2008) and later budesonide (Nolan et al, 2009). The NPMPs

prepared were shown to have advantageous micromeritic and aerosolisation properties for pulmonary drug delivery.

In this paper we explore the feasibility of producing nanoporous microparticles of the hydrophilic excipient materials, trehalose and raffinose with a view to ascertaining if it is possible to produce NPMPs of these excipients which could then be developed as carriers and stabilisers for incorporated therapeutic proteins. We also undertake a preliminary investigation of the effect of including a model protein, lysozyme, in these NPMPs, to see if composite particles can be produced while still retaining the porous morphology of the systems.

2. MATERIALS AND METHODS

2.1 Materials

d-(+)-trehalose dihydrate, d-raffinose pentahydrate and lysozyme (~50,000 units/mg) raw materials were purchased from Sigma, Ireland. Freeze dried lysozyme was prepared as previously described by Chin et al. (1994) and Bromberg and Klibanov (1995). Methanol (MeOH) was purchased from Lab Scan Analytical Sciences, Ireland, while n-butyl acetate (BA) was purchased from Merck, Germany. Ethanol was obtained from Cooley Distillery (Ireland). Deionised water was produced by a Purite Prestige Analyst HP water purification system. Coumarin-6 was purchased from Polysciences Inc, U.S.A. and sulforhodamine 101 was purchased from Fluka, U.S.A. All other reagents were analytical grade.

2.2 Spray drying

All solutions prepared were spray dried with a Büchi B-290 Mini spray dryer. A nozzle tip of 0.7 mm and nozzle screw cap of diameter 1.5 mm were used.

When spray drying aqueous or water/ethanol solutions, the spray dryer was operated in the open mode, whereby the drying gas (compressed air) passes through the drying chamber and then is exhausted. When spray drying all other solutions (containing MeOH/BA), the Büchi B-290 was operated in the closed mode, whereby the drying gas (nitrogen) is recycled to the drying chamber after precooling in a preheat exchanger and solvent condensation in a refrigerator unit (B-295 inert loop). In some cases (as indicated in the text) the high performance efficiency cyclone, designed to improve the separation rate and collection efficiency of particles, was used (Brandenberger, 2003). In all cases the gas flow rate was 670 NI/h (based on air, 4 cm on the gas rotameter indicator), the pump setting was 30% and the aspirator setting was 100%.

In the case of aqueous solutions, trehalose (2% (w/v) solution) and raffinose (2.5 % (w/v) solution) were spray dried at an inlet temperature of 130 °C.

Trehalose was spray-dried as a 0.5% (w/v) solution from ethanol:water comprising 80 or 90% (v/v) ethanol. The solutions also contained ammonium carbonate at a concentration of 10% trehalose content (i.e. 0.05% (w/v) ammonium carbonate). The inlet temperature was 78 or 85 °C.

Trehalose was also spray dried as a 1% (w/v) solution from ethanol:water comprising 60, 70 or 80% (v/v) ethanol, with ammonium carbonate at a concentration of 10 or 25% trehalose content and an inlet temperature of 90 or 95 °C.

A 0.5% (w/v) solution of trehalose and 1% (w/v) solution of raffinose were spray-dried from MeOH:BA in solvent ratios of 50:50, 60:40, 70:30, 80:20 and 90:10 using an inlet temperature of 100 °C.

Freeze-dried lysozyme was spray-dried with trehalose dihydrate at a mass ratio of 1:4 (lysozyme:trehalose dihydrate), from an 80:20 MeOH:BA solvent system and a total solid content (t.s.c.) of 0.5% using an inlet temperature of 100 °C. A high performance cyclone was used.

Freeze-dried lysozyme was also spray-dried with raffinose pentahydrate at a mass ratio of 1:4 from an 80:20 MeOH:BA solvent system and a t.s.c. of 0.5% using an inlet temperature of 100 °C. A high performance cyclone was used to allow comparison with the sugar spray-dried alone.

2.3 Characterisation of physicochemical properties of materials

X-ray powder diffraction (XRD) measurements were made as previously described (Healy et al, 2008). XRD measurements were made on samples in low background silicon mounts, which consisted of cavities 0.5 mm deep and 9 mm in diameter (Bruker AXS, UK). The Siemens D500 Diffractometer used consists of a DACO MP wide-range goniometer with a 1.0° dispersion slit, a 1.0° anti-scatter slit and a 0.15° receiving slit. The Cu anode X-ray tube was operated at 40 kV and 30 mA in combination with a Ni filter to give monochromatic Cu K α X-rays. Measurements were generally taken from 5 to 40° on the two θ scale at a step size of 0.05° per s and were made in duplicate.

Differential scanning calorimetry measurements were carried out under nitrogen purge using a Mettler Toledo DSC 821e (Mettler Toledo Ltd., U.K.) calorimeter. Samples (approximately 4 – 10 mg) were accurately weighed using a Mettler MT50 microbalance into 40 μ l aluminium pans, which were sealed with a lid into which three vent-holes were pierced. A heating rate of 10 °C/min and temperature range of 25 – 200 °C or 25 - 300 °C, was used for all measurements not requiring a heating/cooling step. In some cases a heating/cooling step was carried out either to eliminate overlapping solvent evaporation effects, and involved heating to 100 °C followed by cooling to 70 °C before heating to 200/300 °C as previously stated. Mettler Toledo STAR[®] software was used for capture and analysis of data. At least two measurements were made for each sample.

TGA measurements were carried out on a sample under nitrogen gas purge, using a Mettler TG50 module with attached Mettler MT5 balance (Mettler Toledo Ltd., U.K.). Samples (approximately 4

- 12 mg) were accurately weighed, using a Mettler MT5 microbalance, into 40 μl aluminium pans or lids. Aluminium pans or lids were left open for the duration of the analysis. A heating rate of 10 $^{\circ}\text{C}/\text{min}$ and temperature range of 25-200/300 $^{\circ}\text{C}$, was used for all TGA experiments. Mettler Toledo STAR^c software was used for capture and analysis of data. At least two measurements were made for each sample.

Measurements of particle size distributions were undertaken using a laser diffraction particle sizer - Mastersizer 2000 (Malvern Instruments Ltd., Worcs., U.K.), as previously described (Healy et al, 2008). Dry powders were dispersed using a Scirocco dry powder feeder attachment, using 2 - 3 bar pressure setting and vibration feed rate of 50 - 80% so as to achieve obscuration within the limits of 0.5% - 6%. The particle size reported is the $d(0.5)$, which is the median particle size of the volume distribution. The values presented are the average of at least three determinations. Mastersizer 2000 software was used for analysis of the particle size.

Bulk and tapped density measurements were performed as previously described (Healy et al, 2008). Bulk density (bp) was calculated by determining the weight of powder required to occupy a 1 ml volume in a graduated glass syringe (Lennox Laboratory supplies, Dublin, Ireland), by pouring under gravity. The tapped density (tp) of the powders was determined by vertically tapping this sample onto a level bench-top surface from a height of 5 cm for 100 times. The tapped density was calculated as the ratio of the mass to the tapped volume of the sample. Each measurement was performed in triplicate.

Surface area analyses were performed using a Micromeritics Gemini 2370 analyser, with nitrogen gas (BOC, Ireland) as the analytical (adsorptive) gas and helium (BOC, Ireland) as the reference gas for free space measurements, as required (Nolan et al, 2009). Prior to analysis, samples were degassed under nitrogen gas, using a Micromeritics FlowPrep 060 degasser for 24 hours at 25 $^{\circ}\text{C}$, to remove residual moisture and contaminants. These mild degassing conditions were similar to degassing conditions (25 $^{\circ}\text{C}$ for 16 hours) used by Maa et al. (1999). SEM analysis taken after

degassing ensured that particle morphology was unaffected by the degassing process. Saturation pressure was determined periodically between analyses. The evacuation conditions used were as follows: rate of 500 mmHg/min for 1 minute. Equilibration time for adsorption was 10 s. The amounts of nitrogen gas adsorbed at the relative pressures of 0.05, 0.1, 0.15, 0.2, 0.25 and 0.3 were determined and the BET multipoint surface area was calculated. Where it improved the correlation coefficient for the BET plot, the first or last points were omitted. All analyses were performed in duplicate (two separate samples of powder) and are expressed as the average and range.

Powder samples were visualised using a Hitachi S-4300 field emission scanning electron microscope (Hitachi Scientific Instruments Ltd., Japan) as previously described (Healy et al, 2008). Samples were initially fixed on aluminium stubs using double-sided adhesive tabs. Samples were then sputter-coated with gold. Samples were visualised at 5 kV.

2.4 *In vitro* deposition studies using the Andersen Cascade Impactor (ACI)

Aerodynamic assessment of fine particles was carried out using an Andersen cascade impactor (ACI) and Handihaler device as previously described (Nolan et al., 2009).

Briefly, a size 3 hard gelatin capsule (Farillon Ltd., U.K.) was filled with approximately 25 mg powder, and placed in the Handihaler device (Boehringer Ingelheim, Germany). A pressure drop of 4 kPa was established over the Handihaler device using a Critical Flow Controller Model TPK (Copley Scientific Ltd. UK) and sample collection tube. Flow rate stability was ensured by measuring the absolute pressure on either side of the flow control valve (p_2 , p_3), with a ratio of $p_3/p_2 \leq 0.5$ indicating sonic flow. The flow rate, Q , required to produce a pressure drop of 4 kPa, was measured by attaching a flow meter model DFM2 (Copley Scientific Ltd. UK) in place of the inhaler. A 4 l inspiration volume was achieved by setting the timer so that $t = [4*60/Q]$ s. Two actuations were used to empty the capsule from the Handihaler device, as per the inhaler manufacturer's instructions. The average measured flow produced was ~50 l/min.

After the experiment, retained/deposited powder was collected from the capsule shell, device, mouthpiece, induction port, and each individual stage plus the impaction plate/filter below it, by rinsing and making up to suitable volume with solvent.

In the case of trehalose/coumarin-6 or raffinose/coumarin-6 systems (systems spray dried from MeOH:BA; see section 2.5), the solvent used was 80% (v/v) ethanol/20% (v/v) water, while in the case of trehalose/sulforhodamine 101 or raffinose/sulforhodamine 101 (systems spray dried from water; see section 2.5) the solvent used was water. Mass deposited was calculated from the measured concentration and a prepared standard curve, using fluorescence analysis (as detailed below, section 2.5).

For particles in which lysozyme was incorporated, analysis of the protein was carried out using a Pierce Micro BCA protein assay kit[®] (Pierce, Rockford, IL, USA) (see section 2.6).

The “recovered dose”, being the total amount of powder collected from the device, capsule and impactor was calculated, and the analysis was accepted if this fell within 75% - 125% of the nominal loaded dose (USP, 2008). If the measured recovery was outside the range 75%-125%, the experiment was excluded from the analysis. A table of cumulative mass% (as % of the total recovered emitted dose) versus effective cut-off diameter for each stage of the impactor was constructed. Fine particle fraction (fraction of the emitted dose having aerodynamic diameter < 5 μm) and particle fraction with aerodynamic diameter < 3 μm were calculated by interpolation from the linear portion of the log normal graph of this data. Experimental mass median aerodynamic diameter (MMAD) and geometric standard deviation (GSD) were similarly determined by interpolation from the linear portion of the log normal plot of cumulative mass% (as% of the total dose recovered from the impactor stages) versus effective cut-off diameter.

Analyses were run in triplicate and expressed as mean \pm standard deviation.

2.5 Fluorescence detection

For ACI analyses of trehalose and raffinose powders, a fluorescent marker was incorporated at a low load (0.2% by weight of sugar content) during spray-drying, to enable subsequent quantitation of powder (Bosquillon et al., 2001a, b; Codrons et al., 2003). For porous particles, produced from non-aqueous systems, the fluorescent dye coumarin-6 was used. For non-porous particles, produced from aqueous systems, sulforhodamine 101 was used because of increased water solubility of this marker. Fluorescence measurements were carried out using either an RF 1501 spectrofluorometer with attached sipper unit, or a Fluostar optima microplate reader (BMG Labtech, Germany) using black 96 well flatbottomed plates (Sarstedt, Inc., Germany) and a 200 μ l sample volume, with excitation and emission wavelengths as follows: samples containing coumarin-6 $\lambda_{\text{excitation}} = 485$ nm and $\lambda_{\text{emission}} = 520$ nm; samples containing sulforhadamine 101 $\lambda_{\text{excitation}} = 584$ nm and $\lambda_{\text{emission}} = 612$ nm. All sample and standard measurements were carried out in duplicate. Calibration curves were prepared in triplicate on each apparatus, with the same spray-dried batch of powder and collecting solvent as used in the ACI analysis, and was either freshly prepared or checked simultaneously with each analysis.

2.6 Lysozyme quantitation

Lysozyme quantitation was carried out using a Pierce Micro BCA protein assay kit[®] (Pierce, Rockford, IL, USA). Standards were prepared using the same solvent system as for the test samples and dilutions for at least 2 standard curves were prepared (range 0.04 – 0.005 mg/ml). The assay was performed following the plate assay protocol recommendations, as provided by the manufacturer. Briefly, 150 μ l of appropriately diluted solutions of test/standard were transferred into a clear flat-bottom 96 well micro-plate (Sarstedt, Inc) in duplicate. 150 μ l of the working reagent was added to each well. Plates were covered, manually shaken and incubated in an oven (economy incubator with fan size 1, Gallenkamp) for 2 hours at 37 °C, and allowed to cool to room temperature. The samples were analysed for a colorimetric change measured as the optical density

(O.D.) at 562 nm using a UV plate reader (Microplate Autoreader EL311, Bio-Tek Instruments, U.S.A.). The O.D. of each sample was compared to the average standard curve, and the concentration of lysozyme was extrapolated from this standard curve.

2.7 Lysozyme activity assay

Activity of lysozyme samples was assessed by a turbidimetric rate determination assay proposed by Shugar (1952), and described by Sigma Aldrich. This method is based on the rate of lysis of a suspension of *Micrococcus lysodeikticus* cells by lysozyme enzyme. Measurements were carried out at 25 °C, pH 6.24, using a Helios UV/Vis spectrometer, with attached Thermo Spectronic Single Cell Peltier (Thermo Electron Corp., U.S.A.). Substrate for the assay (0.015% w/v *Micrococcus lysodeikticus* suspension in 66 mM phosphate buffer pH 6.24), was freshly prepared daily, and stored in a water bath at 25 °C until use. Lysozyme enzyme solution (200-400 units; 0.008 mg/ml) in cold 66 mM phosphate buffer pH 6.24, was prepared immediately before use. 2.5 ml substrate was transferred by pipette to a quartz cuvette and allowed to equilibrate to 25 °C in the spectrometer for 3-4 minutes. 0.1 ml of buffer (blank run)/enzyme solution (test run) was pipetted into the cuvette, capped and mixed by inversion. Absorbance at $\lambda = 450$ nm (A_{450}) was recorded every 30 s for 5 min 30 s. The $\Delta A_{450}/\text{minute}$ was obtained from the average decrease in A_{450}/minute for the linear portion of the plot of A_{450} against time. The biological activity (units/mg solid) of the lysozyme sample was then calculated by the following: [df = dilution factor; 0.001 = change in absorbance as per unit definition; 0.1 = volume (in millilitre) of enzyme solution used]

$$\text{Units/ml test solution} = \frac{(\Delta A_{450}/\text{minute Test} - \Delta A_{450}/\text{minute Blank})(df)}{(0.001)(0.1)}$$

$$\text{Units/mg solid} = \frac{\text{units/ml test solution}}{\text{mg solid/ml test solution}}$$

Protein concentration in the test solution was assessed by BCA protein quantitation using a Pierce Micro BCA protein assay kit (Section 2.6).

2.8 Stability studies

Solid state stability studies were conducted using the conditions of temperature and humidity recommended in the ICH protocol for long-term testing, i.e. 25°C/60% relative humidity (RH) (ICH, 2003). Solid samples were placed in open jars in a glass chamber containing a saturated solution of sodium bromide to maintain a constant RH of 60% (Nyqvist, 1983). The glass chamber was stored at 25°C in an incubator (Gallenkamp, UK).

Samples were also stored at refrigerator temperature of 4 °C in a sealed desiccator containing silica gel desiccant and at 25 °C in a sealed desiccator containing silica gel desiccant. At appropriate time intervals, samples were removed for subsequent analysis.

3. RESULTS AND DISCUSSION

3.1 Spray drying trehalose and raffinose from water to produce non-porous microparticles

Spray drying of trehalose from aqueous solution resulted in spherical particles with the majority of particles having wrinkled surfaces (Figure 1(a)), while spray drying of raffinose resulted in spherical particles with smooth surfaces (Figure 1(b)). The differences in particle morphology may be as a result of different T_g s and solubilities for the two materials, both parameters which can influence the morphology of spray dried particles (Masters 1991). There was no evidence, observed from SEM, of shattered or fractured particles. The majority of particles viewed by SEM were less than 5 μ m in diameter.

3.2. Spray drying trehalose to produce NPMPs

3.2.1. Spray drying from ethanol:water solutions

Trehalose:ammonium carbonate solutions were initially spray-dried from 80% (v/v) ethanol or 90% (v/v) ethanol solutions at an inlet temperature of 78 °C, and also from 80% (v/v) ethanol at a higher inlet temperature of 85 °C. The trehalose concentration in solution was 0.5% (w/v) and ammonium carbonate comprised 10 % of solid content. These conditions were chosen based on the solutions which resulted in the successful production of NPMPs of either bendroflumethiazide (Healy et al, 2008) or budesonide (Nolan et al, 2009).

Collected products from these systems were non-free flowing and tended to adhere to the inner wall of the product collection vessel, making further characterisation difficult. Scanning electron micrographs showed fused particles, an example of which is shown in Figure 1(c).

Strategies considered to improve product yield and powder characteristics were alteration of the ethanol concentration (from 60 to 80% (v/v)) and the use of higher inlet temperatures (90-95 °C). Total solid concentration was increased to 1% w/v to increase the product yield. The ammonium carbonate concentration was altered from 10 to 25% of total solid content, to examine any effect on particle morphology.

Spray-dried powders, produced using the higher inlet temperatures of 90-95 °C, did not adhere as strongly to the collection vessel and comprised non-porous spheres and shattered particles, when viewed under SEM. Fusion between particles was reduced compared to the lower inlet temperatures of 78 and 85 °C used. Shattering and fracture of particles was more evident from SE micrographs of trehalose spray-dried with the higher AC content of 25% of total solid content (Figure 2). Particles appeared to be hollow and consisted of thin walls, as observed from these shattered particles.

Thus the ethanol: water:ammonium carbonate system did not produce NPMPs of the hydrophilic sugar.

3.2.2 Spray drying from MeOH: BA solutions

In the case of the previously reported processes for the production of NPMPs of bendroflumethiazide and budesonide, the mixed solvent system which resulted in the production of porous microparticles consisted of a more volatile component which is a good solvent for the processed material and a second, less volatile component which is a poor solvent for the processed material. The process depends on the differences in volatility of the solvent/antisolvent combination used.

The hydrophobic/hydrophilic nature of the compound drug under investigation is an important factor in selecting the solvent system for spray drying to produce NPMPs. Spray drying from an alcohol/water solvent system resulted in the production of NPMPs from bendroflumethiazide and budesonide, both of which are practically insoluble in water, hydrophobic compounds. In these cases ethanol was the solvent and water the antisolvent for the drug. However, trehalose is a hydrophilic, water soluble material, and in this case the solvent/antisolvent system must be adjusted. A MeOH:BA mixed solvent system was chosen, whereby MeOH, the more volatile component (boiling point 65 °C), will now be the solvent and BA (boiling point 126 °C) the antisolvent for the material to be spray dried.

A 0.5 % solution of trehalose was spray-dried from MeOH:BA in solvent ratios of 50:50, 60:40, 70:30, 80:20 and 90:10 using an inlet temperature of 100 °C. Spray-drying was carried out in the closed blowing mode configuration, using nitrogen as the drying gas, due to safety requirements while spray-drying with these organic solvents. Spray-drying resulted in NPMPs as shown in Figure 3. NPMPs spray-dried from different solvent ratio systems showed a similar morphology, which resembled fused nanoparticles.

It was found that spray drying from a 90:10 solvent ratio gave porous particles which were irregular in shape, while spray drying from all other solvent ratios produced porous spheres less than 5 µm in diameter (Figure 3).

It is postulated that the process whereby NPMPs form is similar to that for the model hydrophobic drug compounds previously studied (Healy et al., 2008; Nolan et al., 2009). During the atomisation stage of the spray-drying process, droplets are formed containing the sugar in the co-solvent mix. Rapid drying of these droplets proceeds on contact with the warm drying gas and the more volatile solvent phase (MeOH with a boiling point of 65 °C) in which the sugar is more soluble, evaporates to a greater extent, resulting in the droplet becoming richer in the less volatile solvent component (BA with a boiling point of 126 °C), in which the sugar is less soluble. The fall in the solubility of the sugar may be dramatic and it may condense out initially as a nanosized liquid phase within the droplet. As drying proceeds and further solvent loss occurs, the sugar phase droplets become less fluid and come closer together, and the sugar may precipitate out as primary nanoparticles which agglomerate together either at the particle surface (forming an outer shell) or within the particle, leading to nanoparticulate microparticle formation.

3.3. Spray drying raffinose to produce NPMPs

Given the positive results with trehalose, it was decided to investigate spray-drying of the trisaccharide, raffinose, from similar non-aqueous MeOH: BA solvent systems. Raffinose was spray dried as a 1% (w/v) solution from an 80:20 MeOH: BA solvent ratio system.

NPMPs of raffinose were produced with similar morphology to the trehalose particles and the microparticles were composed of a collection of spherical nanoparticles. The question as to whether particles were hollow was examined by considering all SE micrographs. Evidence of shattered or broken particles was scarce, and particles were generally observed to be intact. SEMs indicated that particles did not appear to be hollow, but were comprised of fused spherical nanoparticles throughout the microparticle.

The effect of changing solvent ratio on the morphology of the particles was examined, and solvent ratios of 90:10, 70:30, 60:40, 50:50 MeOH: BA were investigated.

Addition of BA to raffinose dissolved in the MeOH component in the systems of solvent ratios 60:40 and 50:50 (MeOH: BA) resulted in a phase separation/precipitation of raffinose, and were spray-dried as such with nozzle cleaning set at level 2. The other solvent ratio systems (90:10, 70:30) were spray-dried as solutions. As was found with similar experiments involving spray-drying trehalose, irregular-shaped NPMPs were produced from the 90:10 solvent ratio systems and spherical NPMPs were produced from the 70:30, and 60:40 solvent ratio systems. The presence of some fused and non-porous microparticles amongst NPMPs was noted in the case of raffinose spray-dried from the 60:40 solvent ratio system. This was found to a much greater degree in the 50:50 solvent ratio system.

3.4. Spray drying raffinose:lysozyme and trehalose:lysozyme to produce NPMPs

Lysozyme was used as a model protein to investigate if a protein could be incorporated into sugar-based NPMPs while still retaining the porous morphology.

Lysozyme was used in the freeze-dried form to optimise its solubility in MeOH (Chin et al., 1994; Bromberg and Klivanov, 1995). Freeze dried lysozyme was spray dried from MeOH: BA solution, also containing a sugar, either trehalose or raffinose, in solution.

Particles of spray-dried composite material comprising lysozyme: trehalose (1:4) consisted of porous spheres as seen from SE micrographs (Figure 4a). The pores were smaller (approximately < 90 nm) compared to trehalose spray-dried alone which had a looser nanoparticulate appearance, with surface gaps/pores between nanoparticles approximately < 300 nm (Figure 3).

Spray-dried lysozyme: raffinose (1:4) particles were spherical and porous (Figure 4b). As was observed for the lysozyme:trehalose composite systems, surface gaps/pores were smaller than for the sugar spray-dried alone.

3.5 Physicochemical characterisation of unprocessed and spray dried sugars

3.5.1 Unprocessed trehalose dihydrate

The DSC scan (Figure 5a) showed endothermic peaks - the first at $\sim 91\text{-}97$ °C and the second at $\sim 206\text{-}211$ °C. The first endotherm, at $\sim 91\text{-}97$ °C, can be attributed to loss of the dihydrate, the second endotherm at $206\text{-}211$ °C to melting of the anhydrous β crystal form (Taylor et al., 1998; Ohashi et al, 2007). Mass losses of $\sim 9.5\%$ were calculated from TGA, occurring in one stage. This level of mass loss was close to the theoretical value of 9.5% for the dihydrate sugar. XRD analysis showed characteristic peak positions (at $\sim 9^\circ 2\theta$, $24^\circ 2\theta$) which were consistent with published peak positions for the dihydrate crystal form ($8.7^\circ 2\theta$, $23.8^\circ 2\theta$) (Furuki et al., 2005; Kilburn et al., 2006; Ohashi et al, 2007).

3.5.2 Trehalose spray dried from water (“non-porous spray dried trehalose”)

The powder spray-dried from an inlet temperature of 130 °C was amorphous, as assessed by XRD, which was characterised by the absence of any sharp distinguishing peaks. A broad endotherm was seen from $25\text{-}\sim 100$ °C in the DSC scan, indicative of moisture loss. A transition ascribed to the Tg was identified at ~ 120 °C on the DSC scan but a recrystallisation peak was not identified (Figure 5b). The melting endotherm of anhydrous trehalose at ~ 210 °C was considerably smaller ($\Delta H = 0.74$ J/g) than the unprocessed material ($\Delta H = 125$ J/g). Mass loss over the temperature range $25\text{-}100$ °C from TGA of $\sim 3.6\%$ was consistent with residual moisture or solvent loss.

3.5.3 Trehalose spray dried from ethanol:water

Fused particles spray-dried from the lower inlet temperatures of 78 or 85 °C were not examined due to the sticky nature of the powders. The results presented relate to trehalose samples spray-dried from ethanol:water solutions at the higher inlet temperatures of $90\text{-}95$ °C. Powders were mainly amorphous as confirmed by XRD, although one sample showed a small peak at $\sim 24^\circ 2\theta$, indicative of the dihydrate form of trehalose. This sample had been spray-dried from 60% ethanol with

ammonium carbonate at a concentration of 25% of total solid content and at the higher inlet temperature (95 °C). DSC traces (Figure 5c) were similar for all systems, except for the samples spray-dried from 80% ethanol, inlet temperature 90 °C which showed a jagged pattern between 120-140 °C and a large melting endotherm, consistent with anhydrous trehalose, at ~210 °C ($\Delta H = 131$ J/g) (Figure 5c(v)). Glass transitions were identified at ~120 °C, no recrystallisation exotherms and small or absent melting endotherms were noted, except for the sample spray dried from 80% ethanol at 90 °C. Trehalose spray-dried from 60% ethanol with ammonium carbonate 25% of total solid content (inlet temperature 95 °C), additionally showed an earlier small endotherm in the DSC superimposed on the broad endotherm at ~88 °C (Figure 5c(ii)). This small depression and the evidence from XRD analysis suggest an amount of dihydrate material present in the mainly amorphous sample (for which a T_g was detectable). This may have occurred as a result of processing or following conversion on exposure to ambient temperature and humidity conditions during sample preparation.

Residual moisture or solvent contents of 5-8% were calculated from TGA data. Samples, spray-dried from 70-80% ethanol, 10% of total solid contents of ammonium carbonate, inlet temperature 90 °C, showed a further small mass loss from 100 – 125 °C.

3.5.4 Trehalose spray dried from MeOH:BA

XRD analysis showed that NPMPs of trehalose were amorphous (Figure 6a(i)). A broad endotherm was observed in the DSC of from 25-~120 °C, indicative of solvent or moisture loss (Figure 5d). T_g could be determined from DSC data at ~120 °C in most cases but in some batches was obscured due to the broad endotherm. Melting endotherms consistent with anhydrous trehalose at ~218 °C were identified. Residual solvent or moisture contents of ~3-4% were calculated from TGA (Figure 6b(i)).

3.5.5 Unprocessed raffinose pentahydrate

XRD analysis confirmed the crystalline pentahydrate nature of the unprocessed material by comparison of peaks to published XRD scans (distinct peaks were identified at 10.75, 13.65 and 21.1 °2 θ) (Leinen and Labuza, 2006; Bates et al., 2007).

TGA showed a large step decrease in mass over the temperature range 25- ~130 °C of ~14%. The theoretical stoichiometric mass loss from dehydration of the pentahydrate form is 15%. A sharp endotherm was found in DSC analysis at ~84 °C corresponding to dehydration (Figure 7a). This was followed by an area of disordered pattern, starting at ~110 °C, suggestive of structural collapse or caramelisation of the sugar. No clear endothermic melting peak was observed from DSC. Moura Ramos et al. (2005) reported a similar pattern in the DSC of crystalline raffinose pentahydrate, and explained that raffinose pentahydrate dehydrated at ~80 °C, causing collapse into an amorphous form, and thus no endothermic melting peak was observed. They also found that no crystallisation was found on cooling raffinose in the metastable liquid form.

3.5.6 Raffinose spray dried from water (“non-porous spray dried raffinose”)

XRD analysis demonstrated that raffinose, spray-dried from water (inlet temperature of 130 °C), was amorphous. DSC analysis (heating scan 25-300 °C) showed a broad endothermic peak from 25- ~130 °C followed by decomposition at ~220 °C (Figure 7b(ii)). The broad endotherm obscured the possible identification of a T_g expected at ~ 115-120 °C. Heating to 100 °C (~15 °C below the T_g, to try to remove some of the residual moisture) followed by cooling to 70 °C and reheating to 300 °C, showed a T_g at ~115 °C (Figure 7b(i)). TGA showed ~3.7 % mass loss over the temperature range 25-100 °C, indicative of residual water.

3.5.7 Raffinose spray dried from MeOH:BA

NPMPs of raffinose, spray-dried from the 80:20 MeOH:BA solvent system, were amorphous by XRD, as demonstrated by the absence of any distinguishing peaks and a broad diffuse halo pattern (Figure 6a(ii)).

Fused particles produced from the 50:50 MeOH:BA solvent ratio system were also amorphous, showing a very similar XRD pattern. DSC showed similar patterns for both systems with an initial broad endothermic peak and T_g at ~120 °C (Figure 7c). A small exotherm was also noted immediately after the T_g, particularly evident in the DSC scan in Figure 7c(ii). This can be attributed to a small recrystallisation event or rearrangement of raffinose molecules. TGA showed mass losses of ~ 4% (Figure 6b(ii)), consistent with residual moisture/solvent loss, with an onset occurring earlier than for hydrate water loss (> ~ 83 °C) on comparison to unprocessed material.

3.6 Physicochemical characterisation and biological activity of NPMPs containing lysozyme

Spray-dried composites (mass ratio 1:4) were amorphous by XRD. Biological activity assay carried out on composite particles of lysozyme:trehalose showed excellent retention of activity, with specific activity of the composite particle similar to the original starting material. Table 1 shows the results for each of the spray-dried composites. The specific activity of all composites was similar and not statistically significantly different from the control (unprocessed lysozyme) (at a significance level of $\alpha=0.05$).

3.7 Micromeritic and *in vitro* deposition characterisation of spray dried materials

Based on the results of experiments with other NPMPs and non-porous materials (Healy et al., 2008; Nolan et al, 2009), NPMPs of the sugars, spray-dried from MeOH: BA systems, were expected to show favourable aerodynamic and micromeritic properties for pulmonary delivery, and to be superior to non-porous particles, spray-dried from water. NPMPs (spray-dried from 80:20 MeOH: BA) and non-porous particles (spray-dried from water) of trehalose and raffinose were thus

compared in terms of particle size distribution via laser diffraction particle sizing, surface area, and bulk and tapped density and *in vitro* deposition using the ACI apparatus.

Particle size distribution results (Table 2) suggested that NPMPs were slightly smaller than non-porous particles. The significantly smallest particle size was found for the batch of trehalose NPMPs studied (significance level $\alpha=0.05$).

NPMPs of the two sugars had similar and very low bulk and tapped densities, which were significantly lower than the respective non-porous particles, by a factor of at least 2. Specific surface area measurements of the two sugars were also significantly higher than the non-porous spray-dried sugar particles, by ~ 40 fold. The low bulk and tapped density and high specific surface area values of NPMPs were anticipated from examination of the particle morphology, comprised of fused nanoparticles with voids between these nanoparticles.

Similarity of particles spray-dried with or without fluorescent markers was ascertained by SEM analysis and by laser diffraction particle sizing. SE micrographs and particle sizing of particles including the fluorescent marker, showed them to be very similar in appearance and size to NPMPs or non-porous particles spray-dried without the fluorescent marker.

ACI analysis was carried out using a Handihaler[®] as a delivery device. The two sugars exhibited a similar deposition pattern (Figure 9), with NPMPs having statistically higher particle fraction $< 5 \mu\text{m}$ and $< 3 \mu\text{m}$ (calculated as % of the emitted dose accounted for), and lower mass median aerodynamic diameter (MMAD) and geometric standard deviation (GSD) values, compared to non-porous particles (Table 3). The difference in MMAD values between NPMPs and non-porous particles contrasted with the much smaller difference between median diameters by volume distribution (determined by laser diffraction), and reflects the fact that MMAD may also be affected by the density, shape and dispersibility and aggregation of the powder. NPMPs and non-porous particles both showed a higher MMAD than measured $d(0.5)$, but NPMPs showed a smaller

difference between the two measures of size. This suggests decreased interparticular interactions and aggregation between particles for NPMPs compared to non-porous particles. The GSD value gives an indication of the variability of the aerodynamic diameter of particles. From this data, NPMPs were less variable than non-porous particles. Analysis of deposition patterns showed that all particles deposited primarily in the mouthpiece adaptor and induction port. After this, NPMPs showed higher deposition on the lower stages 3, 4 and non-porous particles showed higher deposition on the upper stages -1, 0, 1.

Bulk and tapped density measurements showed that the composite NPMPs containing lysozyme had low densities but these were higher than the excipient NPMPs spray-dried alone (Table 4). Specific surface area values were high although they were lower than for the excipients spray-dried alone for the lysozyme:raffinose composite. Similar surface area results were measured for the lysozyme:trehalose composite as for trehalose NPMPs spray-dried alone.

Aerodynamic assessment of fine particle showed that the composite NPMPs had good *in vitro* deposition properties (Table 3). Deposition within the impactor was mainly in the mid and lower stages (stage 3 and 4). High deposition was also observed in the mouthpiece adaptor/induction port. The lysozyme:raffinose composite had a lower particle fraction $< 3 \mu\text{m}$ than the lysozyme:trehalose composite. GSD values, indicative of the spread of the aerodynamic diameter, were similar for both NPMP composites.

3.8 Storage stability of protein:sugar composite NPMPs

Storage at 25 °C / 60% RH for 24 hours for lysozyme:raffinose (1:4) and lysozyme:trehalose (1:4) composites resulted in particle collapse when viewed under SEM (Figure 8a and 8b).

Given the deterioration observed at high relative humidity conditions, the conditions 25°C/desiccant; 4°C/desiccant were selected for a 12-week stability study. Particle morphology of

composite particles was not affected by storage under these conditions, as can be seen by comparison of SE micrographs taken at week 12 (Figures 8c and d, 8e and f), with those of the freshly spray-dried material (Figure 3). All composites remained XRD-amorphous during the 12-week stability study at these conditions. DSC and TGA showed no changes, indicating no crystallisation or increased moisture uptake for any the composites stored under desiccant conditions at 4 °C for 12 weeks. Composites of lysozyme:trehalose and lysozyme:raffinose stored under desiccant conditions at 25 °C for 12 weeks displayed some small changes in the DSC (Figure 10) with small endotherms (~ 70 °C) superimposed on the initial broad endotherms in later weeks, which may be due to adsorbed moisture. Moisture content, calculated from TGA, remained at ~4-5% during the 12 weeks of the study.

Biological activity assay showed good retention of specific activity on storage at 4 °C/desiccant for 12 weeks ($98.2 \pm 7.1\%$ for lysozyme:trehalose and $99.1 \pm 7.1\%$ for lysozyme:raffinose), with no statistically significant change compared to freshly spray-dried material. Storage at 25 °C for 12 weeks also showed that activity was well retained for trehalose ($92.5 \pm 7.1\%$) and raffinose composites ($90.8 \pm 7.1\%$).

4. CONCLUSIONS

Nanoporous/nanoparticulate microparticles of hydrophilic materials, such as trehalose and raffinose, can be produced by spray-drying from MeOH: BA solvent systems. The process of NPMP formation is similar to that previously observed for hydrophobic materials in that it involves the use of a mixture of solvents; the more volatile component (in this case MeOH) being a solvent for the material to be spray dried and the less volatile component (BA) being an antisolvent for the material to be spray dried.

Particles have a surface morphology resembling fused spherical nanoparticles, and do not appear to be hollow, as determined from SEM analysis. NPMPs of trehalose and raffinose were amorphous,

as assessed by XRD. Thermal properties of trehalose, assessed by DSC, were found to depend on spray-drying conditions. This was not found with raffinose, with similar DSC patterns for raffinose spray-dried under different conditions. The Tgs of the spray-dried amorphous forms of the two sugars were high and similar to each other — 124 °C (trehalose) and ~120 °C (raffinose). The Kauzmann temperature is generally accepted as the temperature below which translational and rotational motions cease on pharmaceutically relevant time scales (Hancock et al., 1995) and is estimated to be ~50K below the Tg of the material (Hancock et al., 1995; Zhou et al., 2002). The Tgs were sufficiently high to suggest good physical stability at room temperature (given that the Kauzmann temperature will be ~ 70 °C) and suitability for use as stabilisers for protein formulations.

NPMPs (spray-dried from 80:20 MeOH: BA solvent system) displayed favourable aerodynamic and micromeritic characteristics compared to non-porous particles (spray dried from water), suggesting potential suitability for pulmonary delivery.

Incorporation of a model protein, lysozyme into these sugar-based NPMPs at a sugar:protein weight ratio of 4:1 (spray dried from MeOH: BA) resulted in composite systems with retained protein biological activity and favourable particle characteristics for pulmonary drug delivery, with a high fine particle fraction and particle fraction < 3 µm.

ACKNOWLEDGEMENTS

This work was supported in part by Enterprise Ireland (grant CFTD/06/119) and by Science Foundation Ireland (grants 07/SRC/B1154 and 07/SRC/B1158) under the National Development Plan, co-funded by EU Structural Funds.

REFERENCES

- Adjei, A.L., Gupta, P.K. (Eds), 1997. Inhalation delivery of therapeutic peptides and proteins. New York: Marcel Dekker Inc. pp. xiii-xvii.
- Arakawa, T., Prestrelski, S.J., Kenney, W.C., Carpenter J.F., 2001. Factors affecting short-term and long-term stabilities of proteins. *Adv. Drug Deliv. Rev.* 46, 307-326.
- Bates, S., Kelly, R.C., Ivanisevic, I., Schields, P., Zografi, G., Newman A.W., 2007. Assessment of defects and amorphous structure produced in raffinose pentahydrate upon dehydration. *J. Pharm. Sci.* 96, 1418-1433.
- Bosquillon, C., Lombry, C., Preat, V., Vanbever, R., 2001a. Comparison of particle sizing techniques in the case of inhalation dry powders. *J. Pharm. Sci.*, 90, 2032-2041.
- Bosquillon, C., Lombry, C., Preat, V., Vanbever, R., 2001b. Influence of formulation excipients and physical characteristics of inhalation dry powders on their aerosolization performance. *J. Control. Rel.*, 70, 329-339.
- Brandenberger, H., 2003. Development of a novel high-performance cyclone to increase the yield in a mini spray dryer. *Best@buchi Evaporation Inf. Bull.* 27.
- Bromberg, L. E., Klibanov, A. M., 1995. Transport of proteins dissolved in organic solvents across biomimetic membranes. *Proceedings of the National Academy of Sciences USA*, 92 (1995) 1262-1266.
- Carpenter, J. F., Crowe, J. H. 1988. The mechanism of cryoprotection of proteins by solutes. *Cryobiology*, 25, 244-255.

Carpenter, J. F., Crowe, J. H. 1989. Infrared spectroscopic studies on the interaction of carbohydrates with dried proteins. *Biochemistry*, 28, 3916-3922.

Chin, J. T., Wheeler, S. L., Klibanov, A. M., 1994. Communication to the editor on protein solubility in organic solvents. *Biotechnology and Bioengineering*. 44,140-145.

Codrons, V., Vanderbist, F., Verbeeck, R. K., Arras, M., Lison, D., Pr at, V., Vanbever, R., 2003. Systemic delivery of parathyroid hormone (1-34) using inhalation dry powders in rats. *J. Pharm. Sci.* 92, 5, 938-950.

Franks, F., Hatley, R. H. M., Mathias, S. F., 1991. Material science and the production of shelf stable biologicals. *BioPharm* 4(9), 38-55.

Furuki, T., Kishi, A. Sakurai, M., 2005. De- and rehydration behavior of α,α -trehalose dehydrate under humidity-controlled atmospheres. *Carbohydr. Res.* 340, 429-438.

Hancock, B.C., Shamblin, S.L., Zografi, G., 1995. Molecular mobility of amorphous pharmaceutical solids below their glass transition temperatures. *Pharm. Res.* 12, 799–806.

Healy, A.M., McDonald, B.F., Tajber, L., Corrigan O.I., 2008. Characterisation of excipient-free nanoporous microparticles (NPMPs) of bendroflumethiazide. *Eur. J. Pharm. Biopharm.* 69, 1182 – 1186.

ICH, (International Conference on Harmonisation) Guideline Specification Q1A (R2), Step 4. Draft, Stability testing of new drug substances and products, 2003.

Kilburn, D., Townrow, S., Meunier, V., Richardson, R., Alam, A., Ubbink, J., 2006 Organization and mobility of water in amorphous and crystalline trehalose. *Nature Materials* 5, 632-635.

Lee, G., 2002. Spray-drying of proteins. In: Carpenter, J. F, Manning, M. C. (Eds), Rational design of stable protein formulations, New York, Kluwer Academic/Plenum Publishers, pp. 135-158.

Liao, Y.H., Brown, M.B., Nazir, T., Quader, A., Martin G.P., 2002. Effects of sucrose and trehalose on the preservation of the native structure of spray-dried lysozyme. *Pharm. Res.* 19, 1847-1853.

Leinen, K.M., Labuza, T.P., 2006. Crystallization inhibition of an amorphous sucrose system using raffinose. *Journal of Zhejiang University Science B* 7, 85-89.

Maa, Y.-F., Nguyen, P.-A., Sweeney, T., Shire, S. J., Hsu, C. C., 1999. Protein inhalation powders: spray drying vs spray freeze drying. *Pharm. Res.* 16, 249-254.

Mansell, P., 2007. Exubera has opened door for pulmonary delivery growth. www.inpharmatechnologist.com (2007) accessed 04/02/10.

Masters, K. 1991. *Spray Drying Handbook*. 5th Edition, Longman Scientific and Technical., London.

Moura Ramos, J.J., Pinto, S.S., Diogo, H.P., 2005. Molecular mobility in raffinose in the crystalline pentahydrate form and in the amorphous anhydrous form. *Pharm. Res.* 22, 1142-1148.

Nolan, L.M., Tajber, L., McDonald, B.F., Barham, A.S., Corrigan, O.I., Healy, A.M., 2009. Excipient-free nanoporous microparticles of budesonide for pulmonary delivery. *Eur. J. Pharm. Sci.* 37, 593-602.

Nyqvist, H. , 1983. Saturated salt solutions for maintaining specified relative humidities. *Int. J. Pharm. Tech. & Prod. Mfr.* 4, 47-48.

Ohashi, T., Yoshii, H., Furuta, T., 2007. Innovative crystal transformation of dihydrate trehalose to anhydrous trehalose using ethanol. *Carbohydr. Res.* 342, 819-825.

Patton, J.S., 1997. Deep-lung delivery of therapeutic proteins. *Chemtech* 27, 34-38.

Patton, J.S., Fishburn, C.S., Weers, J.G., 2004. The lungs as a portal of entry for systemic drug delivery. *Proc. Am. Thoracic Soc.* 1, 338-344.

Shoyele, S.A., Cawthorne S., 2006. Particle engineering techniques for inhaled biopharmaceuticals. *Adv. Drug Deliv. Rev.* 58, 1009-1029.

Scheuch, G., Kohlhaeufel, M.J., Brand, P., Siekmeier, R., 2006. Clinical perspectives on pulmonary systemic and macromolecular delivery. *Adv. Drug Deliv. Rev.* 58, 996-1008.

Shugar, D., 1952. The measurement of lysozyme activity and the ultra-violet inactivation of lysozyme. *Biochimica et Biophysica Acta*, 8, 302-309.

Stevenson, C.L., Harper, N.J., 2005. Exubera: Pharmaceutical development of a novel product for pulmonary delivery of insulin. *Diabetes Technol. Therap.* 7, 896-906.

Taylor, L.S. York, P., 1998. Characterization of the phase transitions of trehalose dihydrate on heating and subsequent dehydration. *J. Pharm. Sci.* 87, 347-355.

United States Pharmacopoeia (USP), United States Pharmacopoeial Convention, Inc., USA, 2008.

Wendorf, J.R., Radke, C.J., Blanch, H.W., 2004. Reduced protein adsorption at solid interfaces by sugar excipients. *Biotechnol. Bioeng.* 87, 565-573.

White, S., Bennett, D.B., Cheu, S., Conley, P.W., Guzek, D.B., Gray, S., Howard, J., Malcolmson, R., Parker, J.M., Roberts, P., Sadrzadeh, N., Schumacher, J.D., Seshadri, S., Sluggett, G.W.,

Zhou, D., Zhang, G.G.Z., Grant, D.J.W., Schmitt, E.A., Physical stability of amorphous pharmaceuticals: importance of configurational thermodynamic quantities and molecular mobility. *J. Pharm. Sci.* 91, 1863-1872.

Table 1. Summary of biological activity assay results for native lysozyme and the co-spray dried samples (excipient:lysozyme composites spray-dried at a mass ratio of 4:1); The standard deviation values are pooled standard deviation %, calculated from the pooled standard deviation of all samples run for the daily assay as a % of control solution.

	Units/ml test solution	Units/mg solid	μg protein/ml test solution	Units/mg protein	% Specific activity
Trehalose:lysozyme	352.9 ± 11.6	8823 ± 290	8.63 ± 0.23	40874 ± 282	$103.9 \pm 4.4\%$
Raffinose:lysozyme	376.7 ± 25.3	9417 ± 631	10.3 ± 1.25	36763 ± 2624	$93.5 \pm 4.4\%$
Control	350.0 ± 18.5	43750 ± 2312	8.9 ± 0.40	39323 ± 855	$100 \pm 4.5\%$

Table 2. Median particle size, d(0.5) (n = 3; mean \pm standard deviation), surface area (n = 2; mean (range)) and bulk and tapped densities (n = 3; mean \pm standard deviation) for NPMP and non-porous trehalose and raffinose.

	NPMPs of trehalose	Non-porous trehalose	NPMPs of raffinose	Non-porous raffinose
d(0.5) (μm)	2.48 ± 0.04	3.17 ± 0.03	2.96 ± 0.05	3.32 ± 0.23
Surface area (m^2/g)	44.485 (44.837, 44.134)	1.096 (1.155, 1.037)	44.302 (43.187, 45.418)	1.068 (0.931, 1.205)
Bulk density (g/cm^3)	0.075 ± 0.001	0.225 ± 0.012	0.080 ± 0.003	0.342 ± 0.007
Tap density (g/cm^3)	0.124 ± 0.001	0.445 ± 0.021	0.122 ± 0.004	0.587 ± 0.024

Table 3. Summary of results of ACI analysis; expressed as mean \pm standard deviation; for NPMPs (n = 4) and non-porous particles (n = 4) of trehalose; NPMPs (n = 6) and non-porous particles (n = 3) of raffinose and NPMPs of trehalose:lysozyme (4:1) (n=3) and raffinose:lysozyme (4:1) (n=3). (MMAD: mass median aerodynamic diameter; GSD: geometric standard deviation).

Particles	% < 5 μm	% < 3 μm	MMAD (μm)	GSD	% emitted (of nominal dose)
Trehalose NPMPs	40.17 \pm 6.76	24.17 \pm 4.86	3.14 \pm 0.62	2.36 \pm 0.32	80.6 \pm 16.1
Trehalose:lysozyme NPMPs	62.34 \pm 3.91	37.20 \pm 3.51	2.77 \pm 0.35	2.03 \pm 0.06	79.2 \pm 0.8
Trehalose Non-porous particles	16.24 \pm 2.70	7.97 \pm 1.88	12.43 \pm 2.30	3.45 \pm 0.40	66.5 \pm 32.7
Raffinose NPMPs	54.80 \pm 11.50	33.56 \pm 8.82	2.68 \pm 0.80	2.12 \pm 0.17	81.2 \pm 11.0
Raffinose:lysozyme NPMPs	50.05 \pm 5.21	27.47 \pm 2.82	2.92 \pm 0.15	2.04 \pm 0.02	84.2 \pm 0.5
Raffinose Non-porous particles	17.66 \pm 1.9	9.51 \pm 1.91	9.15 \pm 0.81	3.56 \pm 0.35	76.2 \pm 7.5

Table 4. Surface area (n = 2; mean (range)) and bulk and tapped densities (n = 3; mean \pm standard deviation) for NPMPs of trehalose:lysozyme (4:1) and raffinose:lysozyme (4:1).

	NPMPs of trehalose:lysozyme	NPMPs of raffinose:lysozyme
Surface area (m ² /g)	43.743 (45.924, 41.562)	25.459 (25.317, 25.601)
Bulk density (g/cm ³)	0.143 \pm 0.008	0.158 \pm 0.010
Tap density (g/cm ³)	0.245 \pm 0.002	0.278 \pm 0.006

Figure 1. SE micrographs of (a) trehalose spray dried from a 2% w/v aqueous solution, with inlet temperature of spray dryer at 130 °C; (b) raffinose spray dried from a 2.5% w/v aqueous solution, with inlet temperature of spray dryer at 130 °C (c) fused particles of trehalose spray-dried as a 0.5% (w/v) solution from a solvent comprising 80% ethanol/20% water, 10% of total solid content ammonium carbonate; inlet temperature 85 °C.

Figure 2. SE micrographs of trehalose spray-dried from ethanol:water:ammonium carbonate systems, all 1% total solid content (t.s.c.), (a) 60% ethanol, 25 % of t.s.c. ammonium carbonate, 90°C inlet drying temperature; (b) 60% ethanol, 25 % of t.s.c. ammonium carbonate, 95°C inlet drying temperature; (c) 70% ethanol, 25 % of t.s.c. ammonium carbonate, 90°C inlet drying temperature; (d) 60% ethanol, 10 % of t.s.c. ammonium carbonate, 90°C inlet drying temperature; (e) 70% ethanol, 10 % of t.s.c. ammonium carbonate, 90°C inlet drying temperature; (f) 80% ethanol, 10 % of t.s.c. ammonium carbonate, 90°C inlet drying temperature.

Figure 3. SE micrograph showing trehalose spray-dried from MeOH:BA in solvent ratios of (a) 90:10, (b) & (c) 80:20, (d) 70:30, (e) 60:40, (f) 50:50; all 0.5% total solid content, inlet drying temperature 100 °C.

Figure 4. SE micrographs of (a) lysozyme:trehalose and (b) lysozyme:raffinose spray-dried at a mass ratio of 1:4 from MeOH:BA (80:20 solvent ratio), inlet temperature 100 °C.

Figure 5. DSC scan of (a) trehalose dihydrate raw material; (b) trehalose spray-dried from aqueous solution inlet temperature 130 °C; (c) trehalose spray-dried from ethanol:water solutions under the following conditions: % ethanol, % of total solid content ammonium carbonate (AC) in solution, inlet temperature (i) 60%, 25% AC, 90 ° C (ii) 60%, 25% AC, 95 ° C (iii) 70%, 25% AC, 90 ° C (iv) 60%, 10% AC, 90 ° C (v) 80%, 10% AC, 90 ° C (vi) 70%, 10% AC, 90 ° C and (d) trehalose spray-dried from 80:20 MeOH:BA.

Figure 6. (a) XRD scans of (i) trehalose and (ii) raffinose NPMPs; (b) TGA scans of (i) trehalose and (ii) raffinose NPMPs spray dried from MeOH:BA (80:20 solvent ratio).

Figure 7. DSC scan of (a) raffinose pentahydrate raw material; (b) raffinose spray-dried from aqueous solution inlet temperature 130 °C, (i) 25-100-70-300 °C at 10 °C/min, (ii) 25-300 °C at 10 °C/min and (c) (i) raffinose spray-dried from 50:50 MeOH:BA and (ii) raffinose spray-dried from 80:20 MeOH:BA.

Figure 8. SE micrographs of composite particles (a) lysozyme:trehalose (1:4) and (b) lysozyme:raffinose (1:4) after 24 hour storage at 25 °C/60% RH; (c) lysozyme:trehalose (1:4) and (d) lysozyme:raffinose (1:4) after 12 weeks at 4 °C/desiccant; (e) lysozyme:trehalose (1:4) and (f) lysozyme:raffinose (1:4) after 12 weeks at 25 °C/desiccant.

Figure 9. Deposition patterns on the stages of the ACI apparatus: a) non-porous (white bars) and porous (dashed bars) trehalose, b) non-porous (white bars) and porous (dashed bars) raffinose and c) composite lysozyme/trehalose (1:4) (white bars) and composite lysozyme/raffinose (1:4) (dashed bars). Calculated as % of emitted recovered dose (mouth – filter).

MA – mouthpiece adaptor, IP – induction port.

Figure 10. DSC scans of composite particles after storage at 25 °C/desiccant (day 1, week 1, week 4, week 8, week 12 in ascending order) of (a) lysozyme:trehalose (1:4) (b) lysozyme:raffinose (1:4); broken line shows freshly spray-dried material.

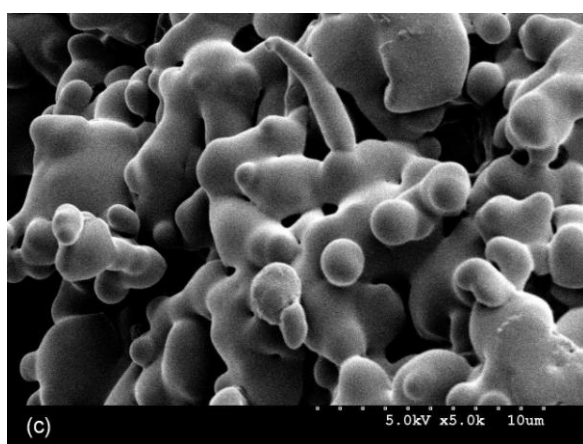
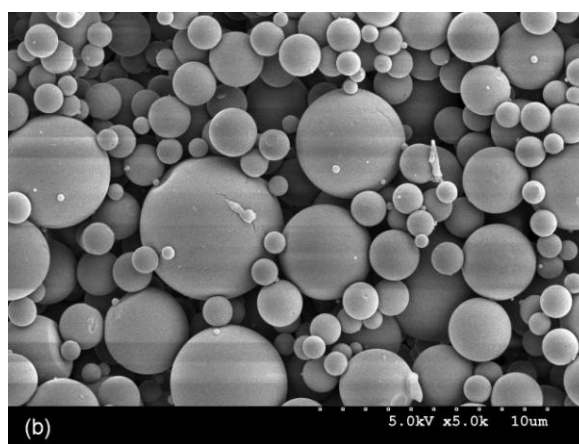
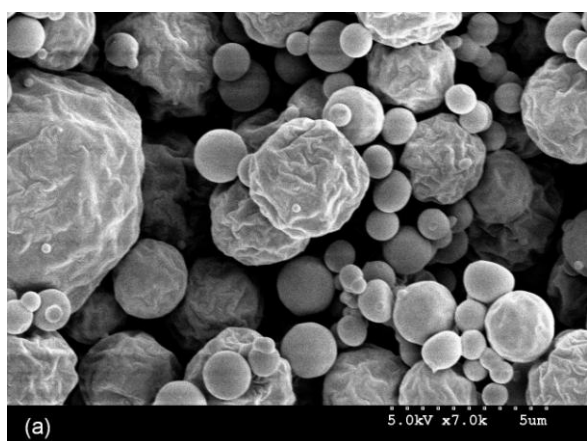


Figure 1.

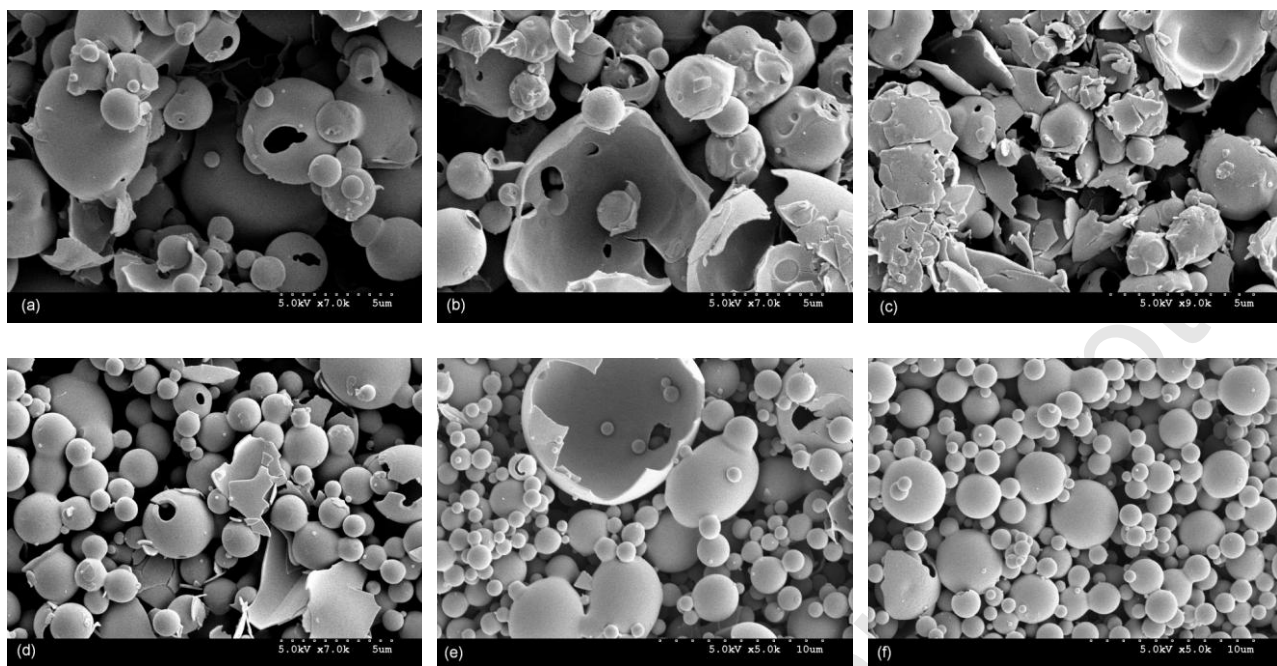


Figure 2

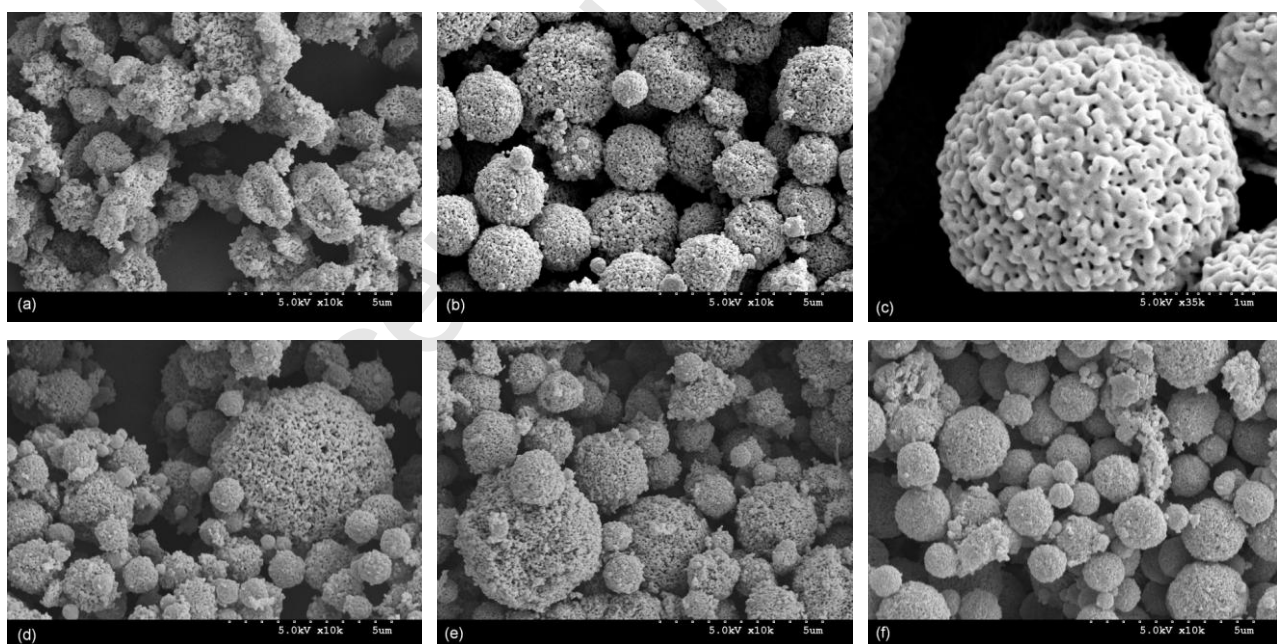


Figure 3.

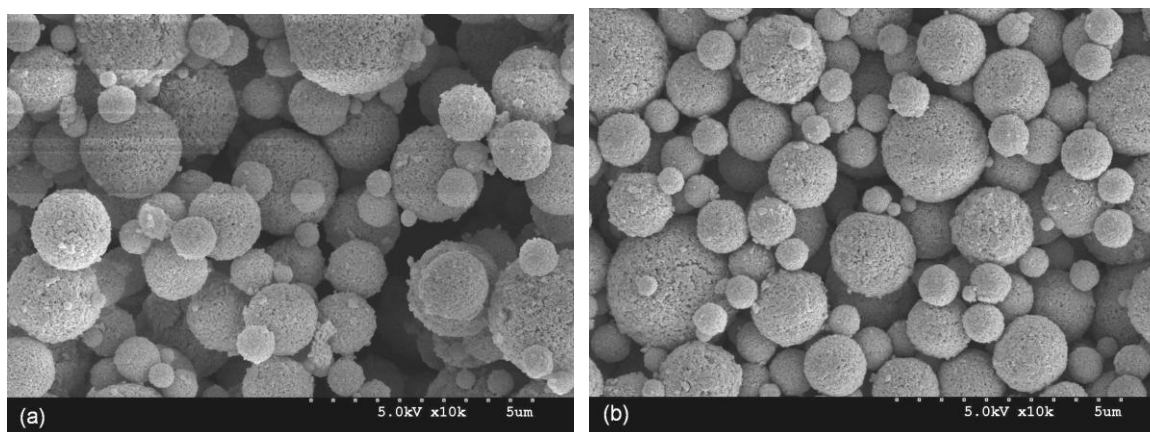


Figure 4.

Accepted Manuscript

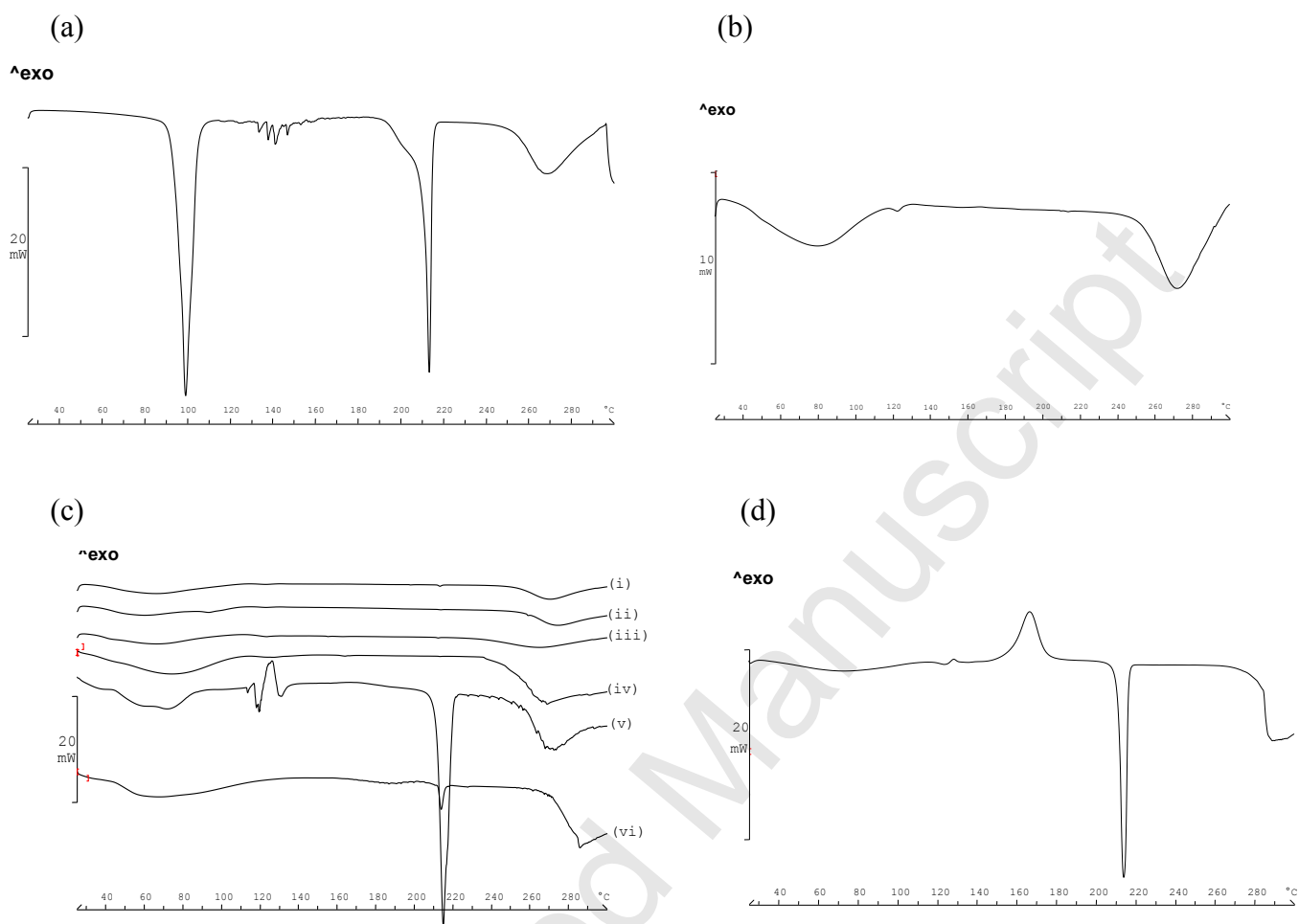


Figure 5.

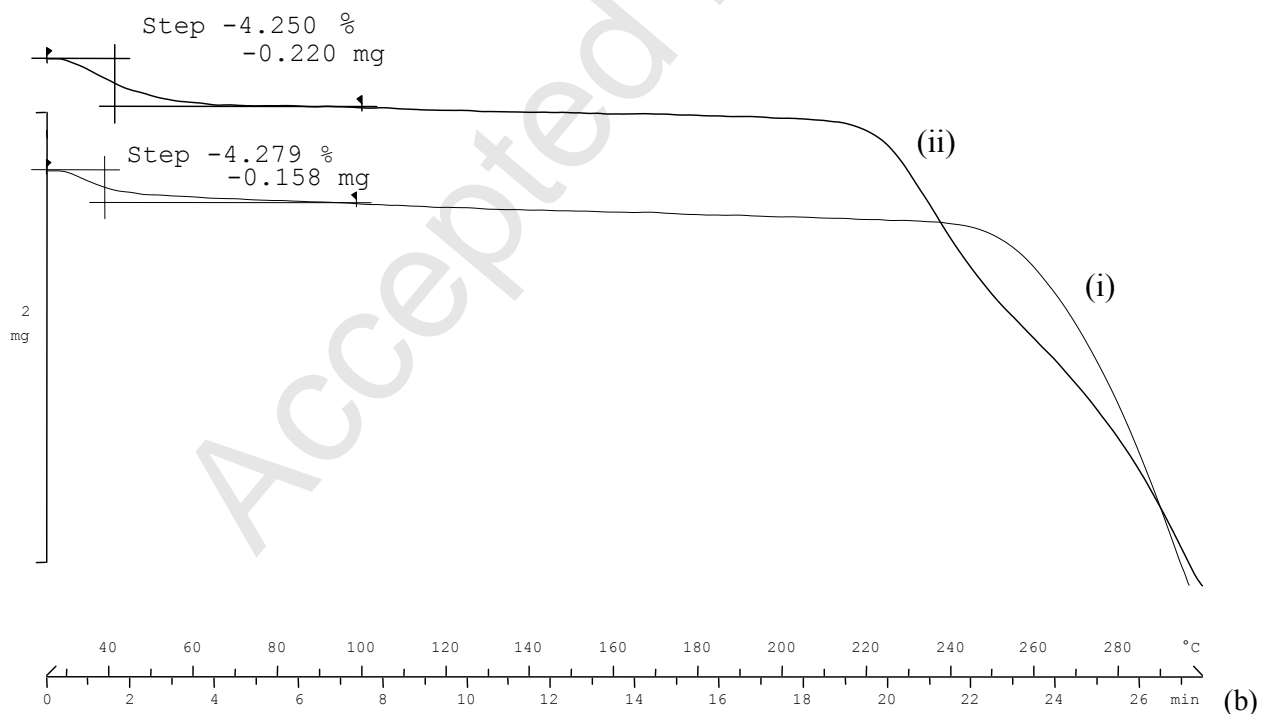
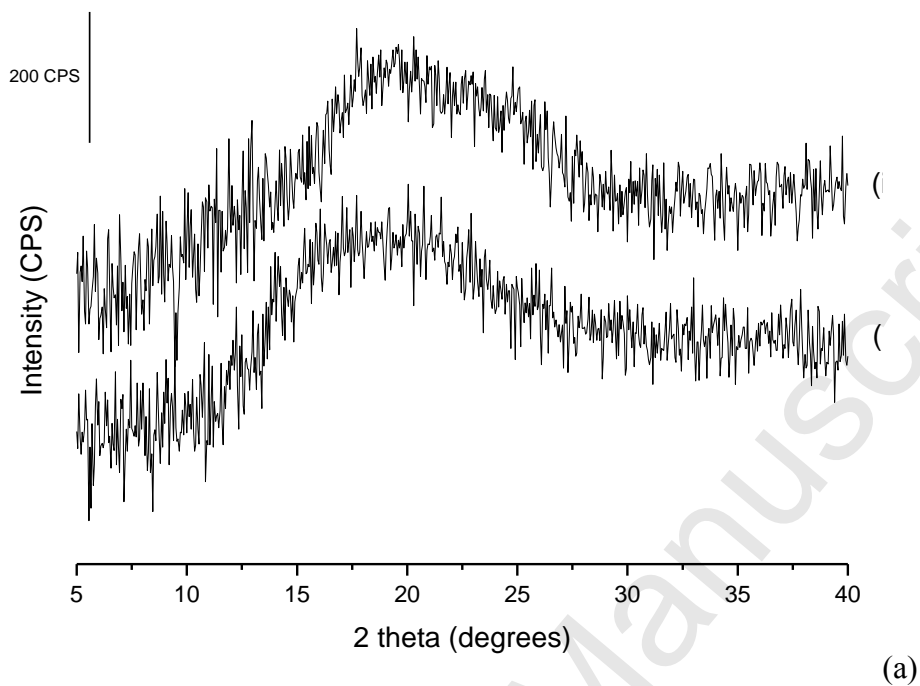


Figure 6.

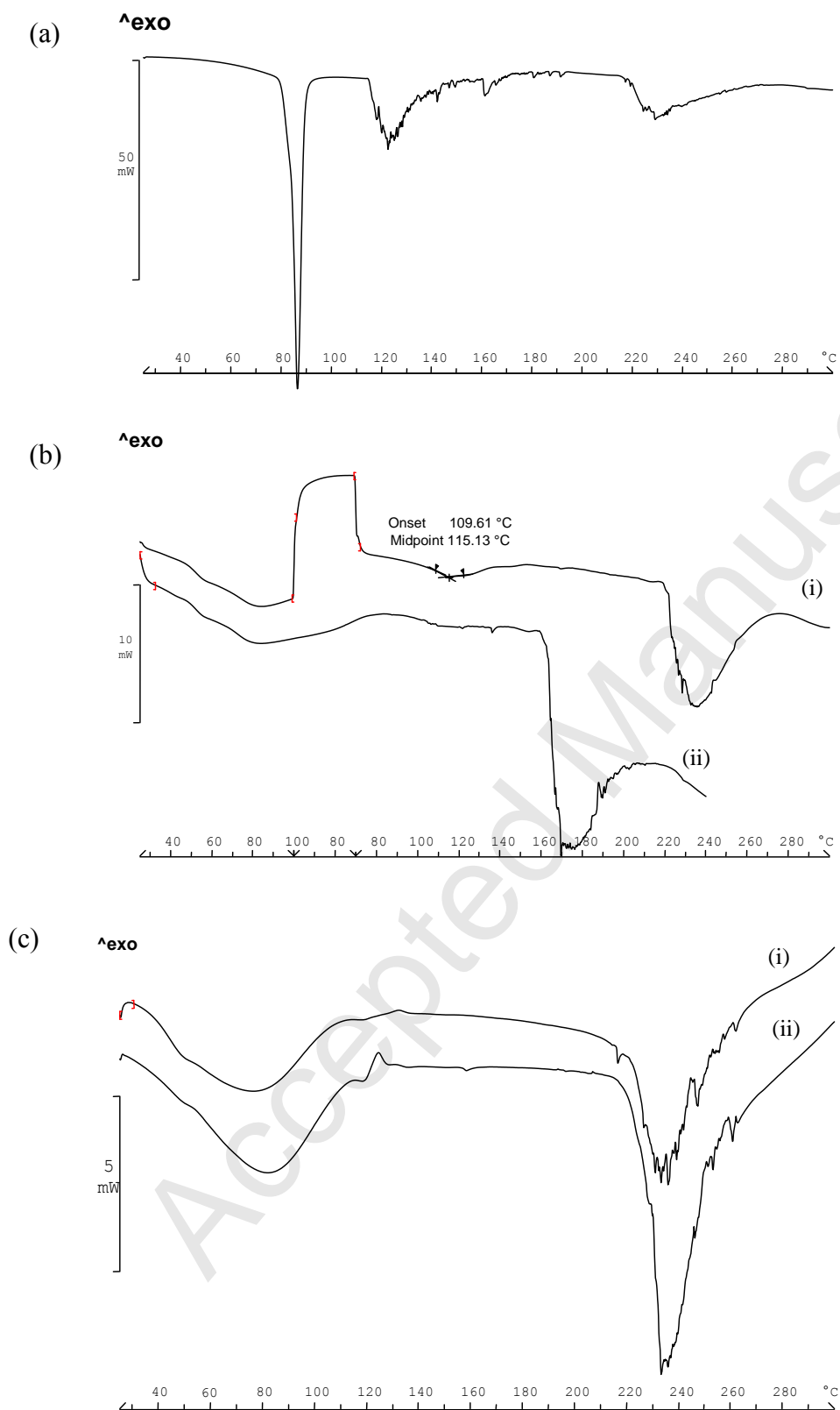


Figure 7.

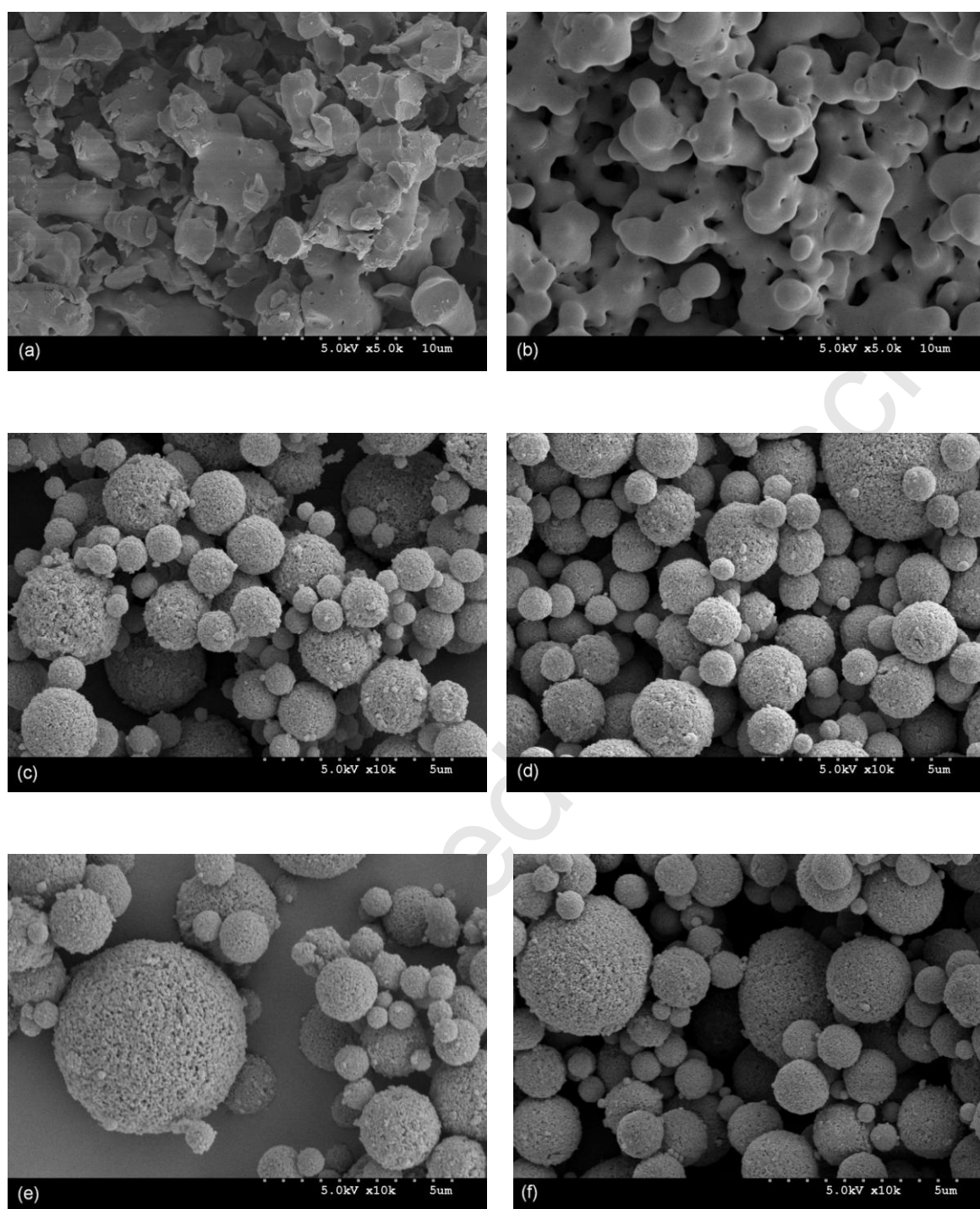


Figure 8.

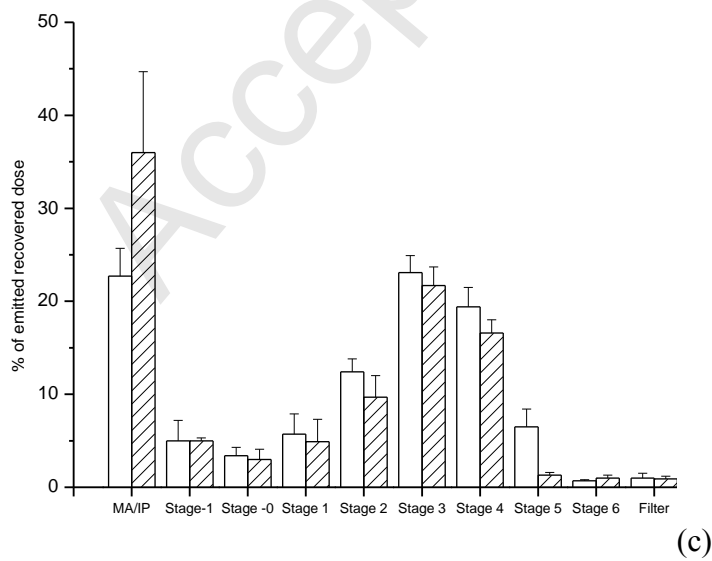
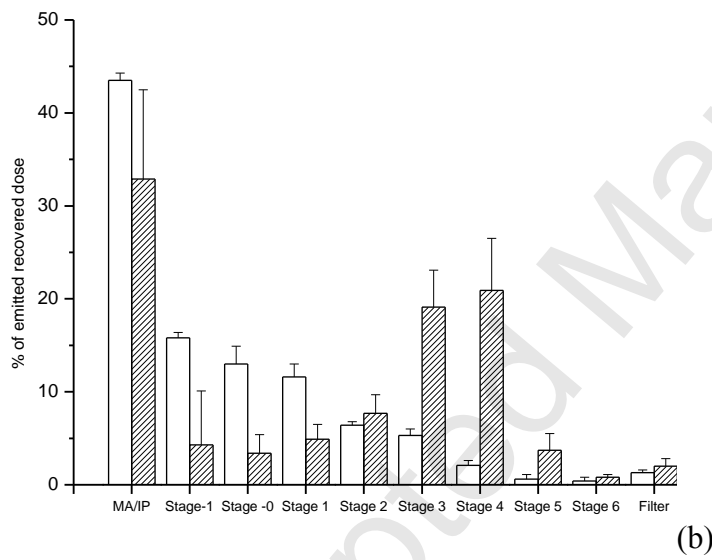
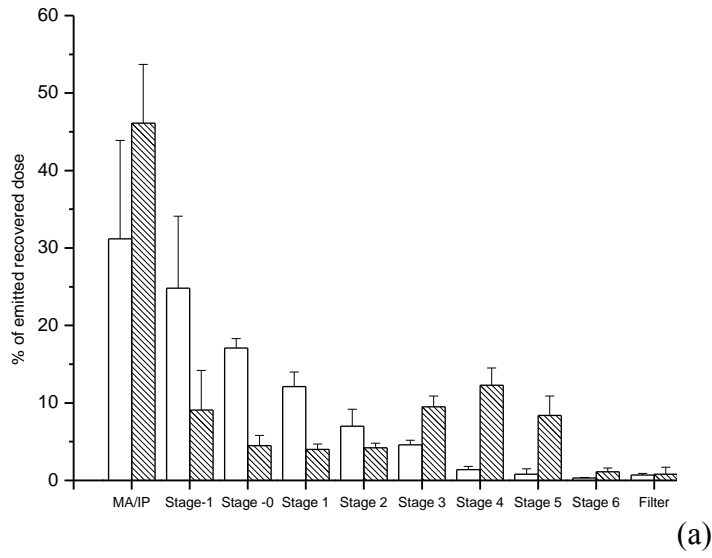


Figure 9.

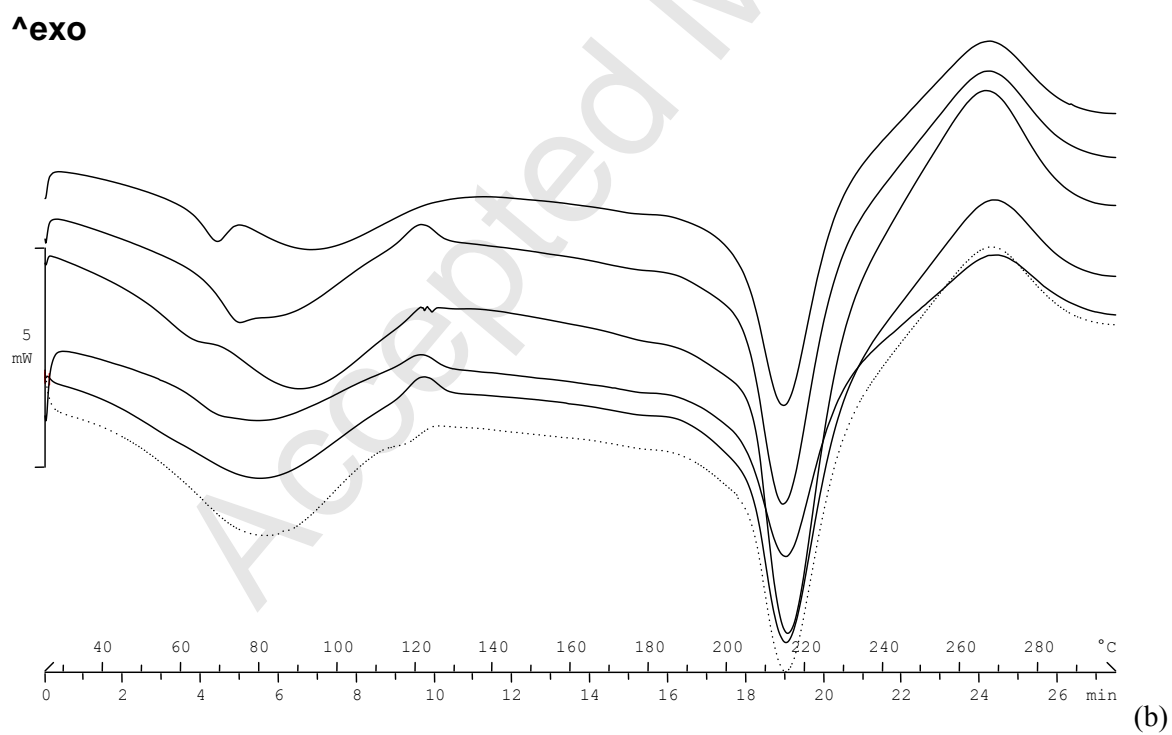
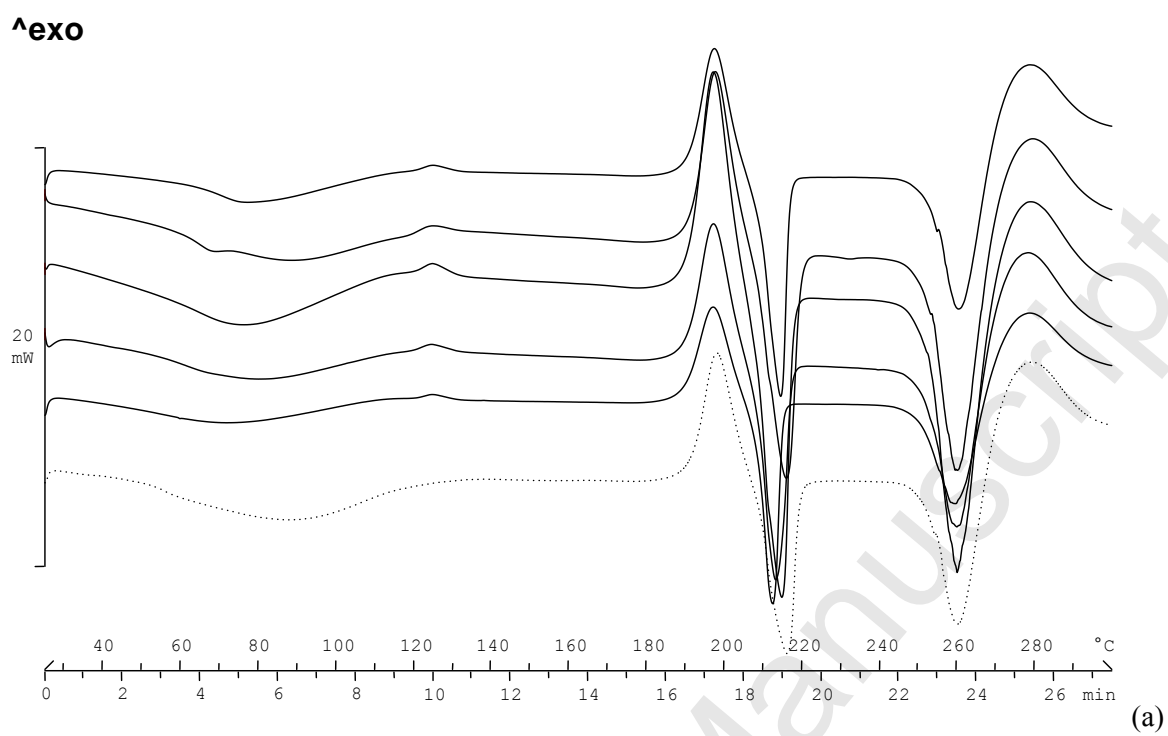


Figure 10.